Available online at www.sciencedirect.com

SCIENCE DIRECT®

Journal of Molecular Catalysis A: Chemical 200 (2003) 251–259

JOURNAL OF MOLECULAR CATALYSIS A: CHEMICAL

www.elsevier.com/locate/molcata

Silica-supported PtSn alloy doped with Ga, In or, Tl Characterization and catalytic behaviour in *n*-hexane dehydrogenation

Narcís Homs[a,*], Jordi Llorca[a], Montserrat Riera[a], Jordi Jolis[a], José-Luis G. Fierro[b], Joaquim Sales[a], Pilar Ramírez de la Piscina[a]

[a] *Departament de Química Inorgànica, Universitat de Barcelona, C/Martí i Franquès 1-11, E-08028 Barcelona, Spain*
[b] *Instituto de Catálisis y Petroleoquímica, CSIC, Campus Universidad Autónoma, Cantoblanco, E-28049 Madrid, Spain*

Received 4 November 2002; received in revised form 24 December 2002; accepted 24 December 2002

Abstract

Silica-supported trimetallic catalysts containing Pt, Sn and a group 13 metal (PtSnM, M = Ga, In, Tl) were prepared by consecutive impregnation steps from *cis*-[$PtCl_2(PPh_3)_2$] and chloride precursors. X-ray diffraction (XRD), transmission electron microscopy (TEM), selected-area electron diffraction (ED) and energy dispersive X-ray analysis (EDX) showed large platelet-like particles of $PtSn_{1-x}M_x$ phases. PtSnGa catalyst with a Pt/(Sn + Ga) molar ratio of 1.72 showed a bimodal particle distribution and a Pt phase was identified. Differences in surface structures were also revealed by the performance of catalysts in the dehydrogenation of *n*-hexane. For PtSnIn and PtSnTl (Pt/(Sn + M) molar ratio of about 1) the dehydrogenation was favoured. In contrast, PtSnGa catalyst yielded hydrogenolysis products. Photoelectron spectra showed the Pt $4f_{7/2}$ level at a binding energy of 70.0–71.8 eV in all cases. Moreover, the FT-IR spectra of chemisorbed CO on the PtSnGa showed a slight shift in the ν(CO) toward higher values with respect to the monometallic catalyst, pointing to an electronic effect in accordance with photoelectron spectroscopy.

Keywords: Silica-supported PtSn; Catalytic behaviour; *n*-hexane dehydrogenation; Doped PtSn alloy

1. Introduction

Platinum-tin catalysts are widely studied in alkane transformation reactions. Platinum-tin combination performs better than platinum alone because the size of platinum ensembles and the bond strength of chemisorbed hydrocarbons may be modified by the addition of tin, which may form an alloy with platinum [1,2]. Moreover, other bimetallic systems such as platinum-indium and platinum-gallium have also shown interesting catalytic behaviour in alkane reactions [3–5]. The introduction of gallium or indium in Pt/Al_2O_3 catalysts improves their stability, increases the selectivity of dehydrogenation reactions and decreases hydrogenolysis [5–8]. A Pt-M interaction has been proposed to be responsible for this change, this behaviour is mainly interpreted as due to a geometric effect. However, in some cases it has been suggested that platinum particles are not modified electronically or geometrically by the presence of gallium [6].

* Corresponding author. Tel.: +34-93-402-1235; fax: +34-93-490-7725.
E-mail address: narcis.homs@qi.ub.es (N. Homs).

1381-1169/03/$ – see front matter © 2003 Elsevier Science B.V. All rights reserved.
doi:10.1016/S1381-1169(03)00040-2

In order to relate the structure of bimetallic Pt-based catalysts to their catalytic behaviour, we have studied tailored Pt-Sn catalysts with well-defined bimetallic phases in hydrocarbon reactions [9,10]. In *n*-hexane reactions, catalysts containing the PtSn phase were stable and favoured dehydrogenation over conversion to benzene and hydrogenolysis [9]. Several attempts to prepare catalysts containing well-defined silica-supported PtGa and PtIn alloys have not allowed the unambiguous characterization of bimetallic phases in the catalyst [11]. However, such catalysts have shown high selectivity in the dehydrogenation of isobutane to isobutene, which has been associated with a change in the properties of alloyed platinum, similarly to Pt-Sn catalysts [12].

Here we examine the performance of silica-supported trimetallic catalysts containing Pt, Sn, and a third element M (M = Ga, In, Tl) in the reactions of *n*-hexane. In an attempt to prepare M-modified PtSn alloys, we used a method which allows us to prepare the well-defined PtSn alloy supported on silica. We relate the catalytic performance to the results of X-ray diffraction (XRD), transmission electron microscopy (TEM), energy dispersive X-ray analysis (EDX), electron diffraction (ED), and X-ray photoelectron spectroscopy (XPS).

2. Experimental section

Catalysts were prepared by successive impregnation of metallic precursors onto Aerosil SiO_2 (Degussa, 200 $m^2\,g^{-1}$) partially dehydrated by treatment under high vacuum at 473 K. First, platinum was incorporated from a methylene chloride solution of *cis*-$[PtCl_2(PPh_3)_2]$. Then, tin was impregnated from an acetone solution of $SnCl_2$. Subsequently, the group 13 metal (Ga, In, Tl) was incorporated from an acetone solution of the respective MCl_3 salt. After each impregnation step, samples were treated under vacuum at 373 K overnight. All catalysts were prepared under air-free atmosphere and reduced under a flow of hydrogen at 673 K for 16 h.

X-ray diffraction patterns were recorded on a Siemens D-500 powder X-ray diffractometer equipped with a graphite monochromator, using Cu Kα (λ = 0.15406 nm). Powder patterns were recorded in the range $2\theta = 20$–80° with a step width of 0.05° and 10 s counting time.

Samples for transmission electron microscopy studies were suspended in methanol and stirred continuously in an ultrasonic bath. The resulting suspensions were placed on copper grids with a holey-carbon-film support, and the alcohol was allowed to evaporate. High-resolution TEM combined with energy dispersive X-ray analysis was performed using a Philips CM-30 electron microscope working at 300 kV and equipped with a Link analytical system. The X-rays emitted upon electron irradiation were acquired in the range 0–20 keV with an 8–10 nm probe. Electron diffraction was carried out in selected-area mode.

Photoelectron spectra (XPS) were acquired with a VG ESCALAB 200R spectrometer equipped with a Mg Kα ($h\nu = 1253.6$ eV, 1 eV = 1.6302×10^{-19} J) X-ray exciting source, a hemispherical electron analyser and a pretreatment chamber. The residual pressure in the ion-pumped analysis chamber was maintained below 4.2×10^{-9} mbar (1 mbar = 101.33 Pa) during data acquisition. The binding energies (BE) were referred to the C 1s peak at 284.9 eV which gave BE values with an accuracy of ±0.1 eV. Peak intensity was calculated as the integral of each peak after smoothing and subtraction of the S-shaped background and fitting of the experimental curve to the sum of Gaussian and Lorentzian lines of variable proportion.

Infrared spectra (FT-IR) were obtained at room temperature on a Nicolet 520 Fourier transform instrument at 2 cm^{-1} of resolution over pelleted samples. For these experiments special greaseless vacuum cells with CaF_2 windows which allowed thermal treatments were used.

Catalytic behaviour in the *n*-hexane reaction was studied in a continuous-flow glass microreactor at atmospheric pressure. Sixty to ninety milligrams of catalyst diluted with SiC was used for each test. Samples were re-reduced in situ at 673 K for 1 h in flowing hydrogen. H_2 was then replaced by an H_2 feed saturated with *n*-hexane (5 ml min^{-1}, H_2:*n*-hexane = 4:1) and *T* was raised to 723 K in 2 h. Products were separated in a TRB-1 capillary column on a gas chromatograph equipped with an automated gas sample valve. *trans*-3-Hexene was not quantified due to its low yield and proximity to the *n*-hexane peak.

Table 1
Chemical analysis and Pt:Sn:M (M = Ga, In or Tl) atomic ratios of silica-supported catalysts

Catalyst	Pt (%)	Sn (%)	M (%)	Pt:Sn:M
PtSnGa	2.80	0.74	0.15	1:0.43:0.15
PtSnIn	2.37	1.07	0.34	1:0.74:0.25
PtSnTl	2.76	1.30	0.43	1:0.78:0.15

3. Results and discussion

3.1. Characterization of catalysts

The catalysts prepared and their metallic content are listed in Table 1. Fig. 1 shows XRD patterns of the catalysts. In all cases, the diffraction peaks correspond to the hexagonal PtSn phase. However, the position of the peaks depends on the atomic volume of the doping metal. When 2Θ values were compared to those of PtSn diffraction peaks, higher values for PtSnGa, lower for PtSnTl and similar values for PtSnIn were observed, according to the incorporation of doping metals to the PtSn phase and the sequence of radius $r_{Tl} > r_{In} \approx r_{Sn} > r_{Ga}$.

The study of PtSnGa catalyst by TEM showed a bimodal particle distribution; large particles had platelet morphology (28 × 7 nm) and small particles (1.2–1.6 nm) were highly dispersed on the silica (see Fig. 2). Individual electron diffraction patterns of the large particles correspond to a hexagonal phase with $a = 4.10$ Å (1Å = 0.1 nm) and $c = 5.41$ Å (inset Fig. 2). EDX analysis of these particles indicated the simultaneous presence of Pt, Sn, and Ga. Taking into account the value of parameters $a = 4.10$ Å and $c = 5.44$ Å for the hexagonal PtSn alloy, a composition $PtSn_{1-x}Ga_x$ is proposed for these particles, also agreeing with the XRD results. On the other hand, the selected-area electron diffraction pattern of this catalyst showed reflections for the $PtSn_{1-x}Ga_x$ alloy and those corresponding to an fcc phase (inset Fig. 2), indicating the presence of $PtSn_{1-x}Ga_x$ and probably Pt phases. The bimetallic or monometallic nature of the small particles could not be established by EDX analysis, since the electron probe used was in the 5–8 nm range. However, taking into account the characterization results mentioned above and the Pt:Sn:Ga atomic ratio of this catalyst (1:0.43:0.15) at least some of the small particles were assumed to be monometallic platinum particles, although the

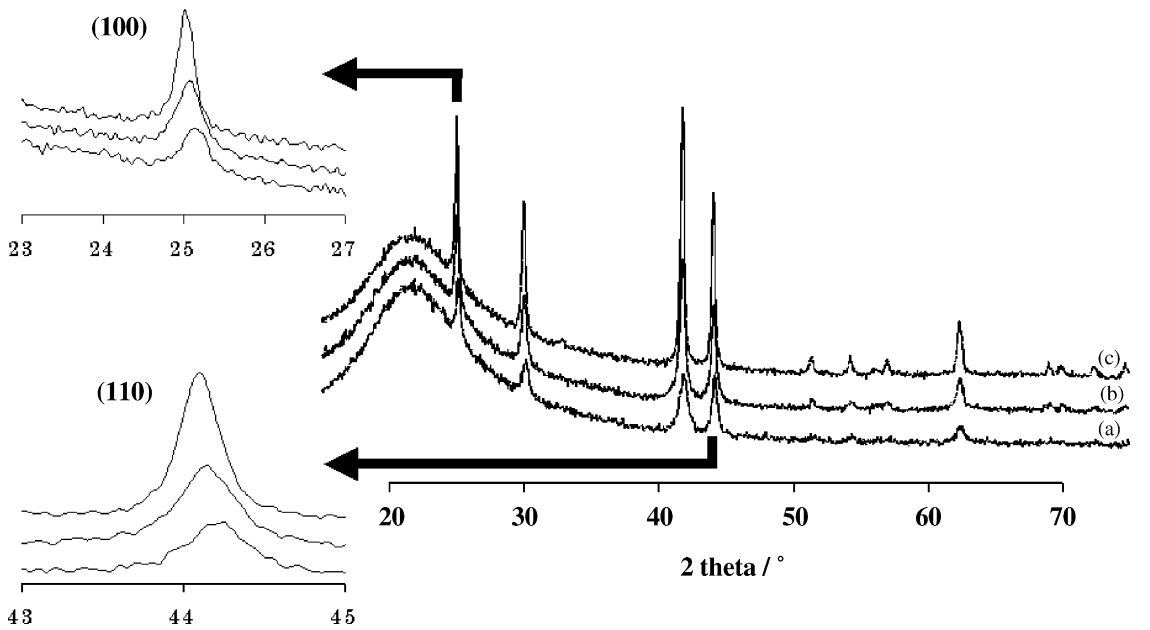

Fig. 1. X-ray diffraction patterns recorded for catalysts: (a) PtSnGa; (b) PtSnIn; (c) PtSnTl.

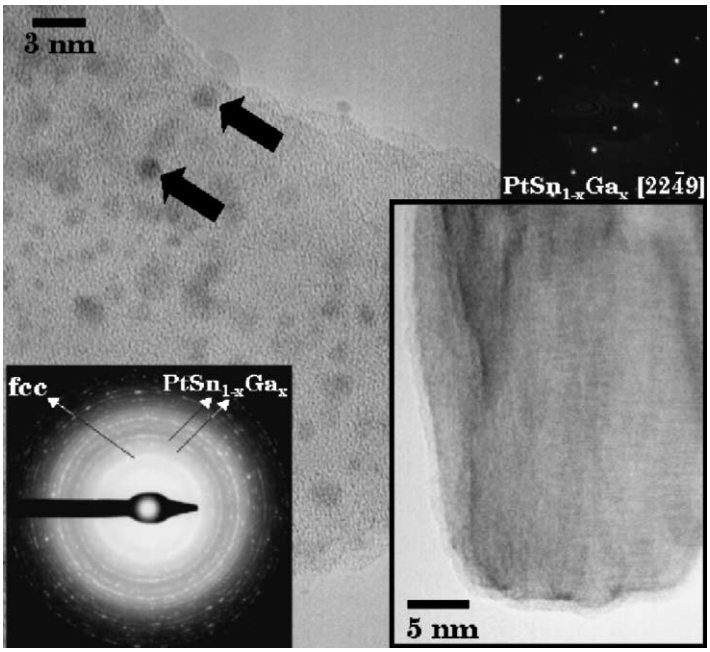

Fig. 2. High-resolution transmission electron microscopy images of the PtSnGa catalyst along with electron diffraction patterns.

presence of bimetallic Pt-Ga particles cannot be ruled out.

Transmission electron micrographs of PtSnIn and PtSnTl catalysts only showed large particles in the 26×6 to 23×7 nm range, with a plate-like structure (Figs. 3 and 4). EDX analysis of these particles indicated a trimetallic composition for both PtSnIn and PtSnTl catalysts. Their selected-area electron diffraction patterns indicated the presence of exclusively hexagonal phases, whereas electron diffraction patterns from individual particles (insets Figs. 3 and 4), allowed us to obtain cell parameters $a = 4.10$ Å and $c = 5.44$ Å for PtSnIn sample and $a = 4.11$ Å and $c = 5.45$ Å for PtSnTl catalyst. In agreement with XRD data, these calculated parameters might be assigned to $PtSn_{1-x}In_x$ and $PtSn_{1-x}Tl_x$ alloys, respectively.

X-ray photoelectron spectra of the Si 2p, Pt 4f, Sn 3d, Ga 2p, In 3d and Tl 4f core levels were recorded. From peak intensities and atomic sensitivity factors [13], surface atomic ratios were calculated (Table 2).

Fig. 5 displays the Pt 4f spectra. In all cases the Pt $4f_{7/2}$ level is deconvoluted into two components: one at low BE centred at 70.0–70.7 eV and the other at higher BE located at 71.2–71.8 eV (see Table 2). Bimetallic Pt-Sn silica-supported catalysts prepared from the same precursors and containing PtSn alloy have shown a single component for the Pt $4f_{7/2}$ level located at 71.2–71.5 eV, while the analogous monometallic Pt/SiO_2 catalyst has shown a single signal at 71.3 eV [9]. However, bimetallic Pt-M (M = Ga, In, Tl) silica-supported catalysts, containing PtM alloys have shown two components for Pt $4f_{7/2}$ level, located at 70.4–71.1 eV and 72.0–72.7 eV [11]. The component at a BE lower than that of Pt 4f in Pt/SiO_2 or $PtSn/SiO_2$ may have been caused by electronic modification of the platinum by a Pt-M interaction. This interaction may be also responsible for the component at 70.0–70.7 eV for the catalysts prepared in this study. This assumption is consistent with the findings of Mériaudeau et al. for Pt_xIn_y in NaY zeolite [3]. These authors found the Pt 4f BE for Pt-In to decrease slightly (0.2 eV) with respect the monometallic Pt catalyst, and an electronic effect in the alloyed platinum was not excluded.

Sn $3d_{5/2}$ peak profiles are complex. On the basis of the shape and width, Sn $3d_{5/2}$ peaks can be deconvoluted into three components (see Fig. 6). The component at lower BE 483.6–484.1 eV, which is the

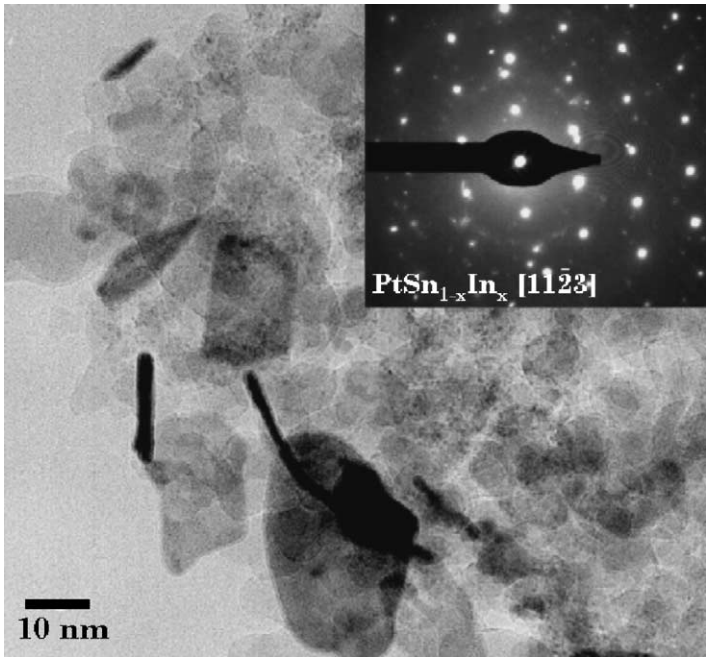

Fig. 3. Bright-field transmission electron micrograph of the PtSnIn catalyst. The inset corresponds to a selected-area electron diffraction of one of the particles.

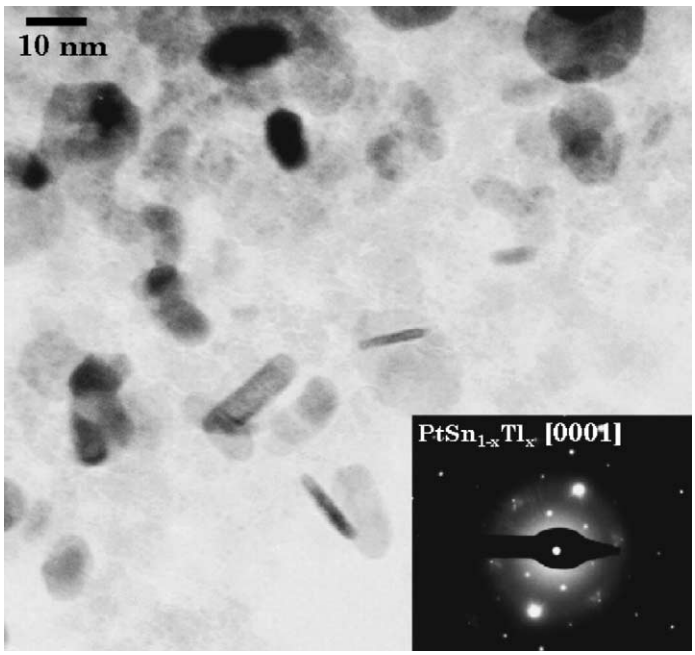

Fig. 4. Bright-field transmission electron micrograph of the PtSnTl catalyst. The inset corresponds to a selected-area electron diffraction of a single hcp $PtSn_{1-x}Tl_x$ particle.

Table 2
Binding energies (eV) of core electrons and XPS atomic ratios for silica-supported PtSnM catalysts

Catalyst	Pt $4f_{7/2}$	Sn $3d_{5/2}$	M[a]	Pt/Si	Sn/Si	M[a]/Si
PtSnGa	70.7 (37) 71.8 (63)	484.1 (17) 485.6 (38) 487.7 (45)	22.5	0.0122	0.0226	0.0135
PtSnIn	70.0 (24) 71.2 (76)	484.0 (17) 484.7 (43) 486.3 (40)	443.7 (57) 444.9 (43)	0.0243	0.0241	0.0073
PtSnTl	70.2 (23) 71.3 (77)	483.6 (16) 485.0 (49) 487.4 (35)	118.4	0.0053	0.0137	0.0030

[a] M corresponds to Ga 2p, In $3d_{5/2}$ or Tl $4f_{7/2}$ levels for samples containing Ga, In or Tl, respectively.

minor one, corresponds to zero-valent Sn, and that located in the range 484.7–485.6 eV, can be assigned to alloyed tin. On the other hand, oxidized tin was also detected on the surface of the catalysts (component at 486.3–487.7 eV). Zero-valent tin, alloyed tin, and oxidized tin had already been detected by XPS in bimetallic PtSn catalysts containing the PtSn alloy [14].

Regarding the values of Ga 2p, In $3d_{5/2}$, and Tl $4f_{7/2}$ levels obtained for PtSnM catalysts (M = Ga, In, Tl), only the presence of a reduced phase was determined

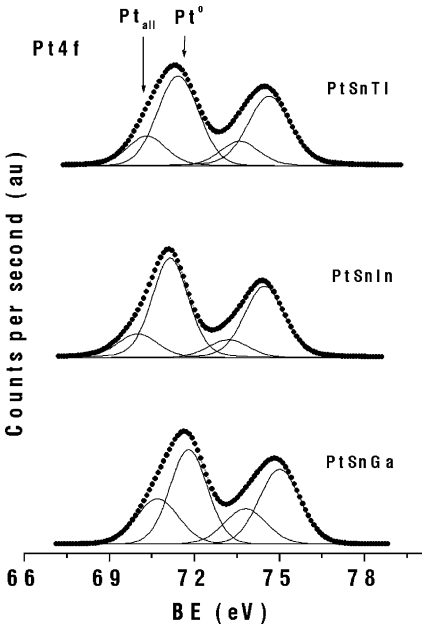

Fig. 5. Pt 4f core level spectra of PtSnM (M = Ga, In, Tl) catalysts.

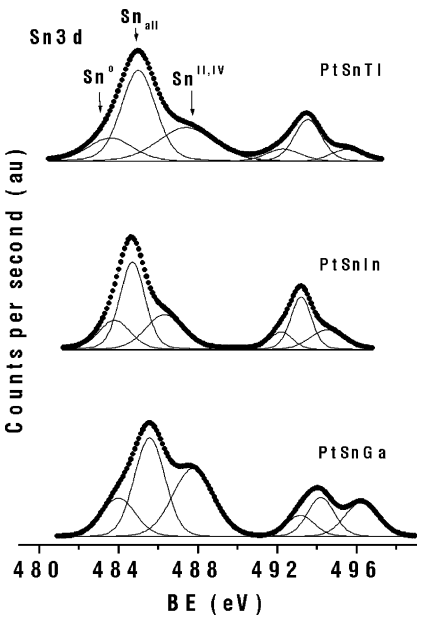

Fig. 6. Sn 3d core level spectra of PtSnM (M = Ga, In Tl) catalysts.

Table 3
ν(CO) (cm^{-1}) for silica-supported catalysts at Θ(CO) = 1 and Θ(CO) = 0

Catalyst	ν(CO) (cm^{-1})	
	Θ(CO) = 1	Θ(CO) = 0
PtSnGa	2073	2060
Pt[a]	2073	2055
PtSn[a]	2061	2054

[a] From [16].

Table 4
Catalytic performance for silica-supported catalysts in *n*-hexane transformation

Catalyst	Time (h)	Activity (mmol h^{-1} g Pt^{-1})	Selectivity/(%)								
			$C_1 + C_5$	$C_2 + C_4$	C_3	Dimethylbutanes	Methylpentanes	Hexenes[a]	MethylcycloC$_5$[b]	Benzene	CycloC$_6$[c]
PtSnGa	0.8	58.2	7.8	13.4	11.5	0.5	15.3	44.2	5.3	1.2	0.8
	1.6	49.5	6.8	11.4	10.0	0.3	13.8	50.4	5.4	1.1	0.8
PtSnIn	0.4	40.7	–	–	2.0	–	–	95.7	–	0.8	1.5
	2	33.4	–	–	1.6	–	–	96.9	–	0.7	0.8
PtSnTl	0.3	11.0	–	–	–	–	–	98.4	–	1.6	–
	1.3	7.8	–	–	–	–	–	100	–	–	–
PtSn	0.3	60.2	–	–	–	–	–	98.9	–	–	1.1
	1	59.3	–	–	–	–	–	98.9	–	–	1.1

5 ml min^{-1}, H_2:*n*-hexane = 4:1, $T = 723$ K.

[a] Includes 1-hexene, *cis*-2-hexene, *trans*-2-hexene and *cis*-3-hexene.

[b] Includes methylcyclopentane and methylcyclopentene.

[c] Includes cyclohexane and cyclohexene.

for indium-modified system. For this catalyst, a 57% of indium determined by XPS was in zero-valent state (BE In $3d_{5/2}$ 443.7 eV).

If the surface atomic ratios derived from XPS are compared with the bulk composition of the catalysts (Table 2), in all cases, Pt/Sn and Pt/M (M = Ga, In, Tl) surface ratios are lower than bulk ratios, which indicates a segregation of Sn and M on the surface of catalysts.

CO adsorption experiments followed by FT-IR were performed with the aim to characterize the metallic particles. In order to avoid any dipole-dipole interaction which might modify the adsorbed ν(CO), the singleton frequency (ν(CO) at Θ(CO) = 0) was determined. For this purpose, we used in this work the method proposed by Primet [15], which consists in recording the spectra of the catalysts exposed to CO from the high coverages until the ν(CO) band disappeared, by outgassing the sample at increasing temperatures. From a plot of the frequency as a function of the CO equilibrium pressure, the extrapolation of the ν(CO) at Θ(CO) = 0 provides the singleton value. This method was used to study the PtSnGa sample (Table 3). Values already reported for related catalysts prepared by a similar method are also included in Table 3 [16]. PtSnGa sample showed a higher ν(CO) singleton than the monometallic catalyst (mean particle size of Pt 1.8 nm) or PtSn sample, in which only the presence of the well-defined PtSn phase (mean particle size along the basal plane of particles 24 nm) was found. As stated above, PtSnGa catalyst showed a bimodal distribution of particles around 28 and 1.4 nm. Taking into account that a small particle size favours the decrease in ν(CO) due to the increase in Pt back donation to the π-antibonding orbital of CO adsorbed [17], the results may indicate an electronic effect in the PtSnGa sample. These results reveal a difference between PtSn and PtSnGa samples and are consistent with XP spectra.

4. Catalytic activity

Table 4 shows the activity and selectivity of different catalysts in the *n*-hexane reactions as well as catalytic data recorded in the same experimental conditions for a bimetallic catalyst containing the well-characterized PtSn alloy. The high stability and selectivity for dehydrogenation of the PtSn catalyst has been related to the presence of the PtSn phase in which a geometric effect for platinum has been shown [9,16].

The PtSnIn and PtSnTl catalysts prepared in this study also showed high selectivity for dehydrogenation according to the characterization results, which show the presence of $PtSn_{1-x}M_x$ as the only active phase. However, the catalytic activity of PtSnTl sample was significantly lower than that of PtSn or PtSnIn samples. A small substitution of Sn by Tl in the PtSn phase had a detrimental effect on the catalytic behaviour. This catalyst showed the lowest Pt/Si and Pt/(Sn + M) surface ratios, probably due to a segregation of Tl on the particle surface.

The selectivity pattern of PtSnGa was very different. The rate of cyclization, and particularly of hydrogenolysis reactions, was high for the PtSnGa catalyst. As discussed above, in the Ga-doped catalyst, both Pt particles and $PtSn_{1-x}Ga_x$ particles were present and the presence of bimetallic Pt-Ga particles could not be ruled out.

5. Conclusion

Silica-supported $PtSn_{1-x}M_x$ particles (M = Ga, In, Tl) were prepared from monometallic precursors. Photoelectron spectra of the Pt $4f_{7/2}$ core level of all the catalysts showed a component at low BE, which can be ascribed to an electronic effect on platinum. This finding is also consistent with CO chemisorption experiments on PtSnGa catalyst. The nature and structure of the metallic phases on the support surface strongly affects the dehydrogenation of *n*-hexane. Samples in which only $PtSn_{1-x}M_x$ phases were identified gave high selectivity to dehydrogenation products, thus indicating a dilution effect of platinum in $PtSn_{1-x}M_x$ particles.

Acknowledgements

We thank CICYT (MAT1999-0477, MAT2002-01739) and CIRIT (2001SGR-00052) for financial support, Johnson-Matthey is gratefully acknowledged for the loan of platinum salt. J. Llorca is grateful to MCYT for a Ramon y Cajal research program.

References

[1] R.D. Cortright, J.A. Dumesic, J. Catal. 148 (1994) 771.
[2] B. Shi, B.H. Davis, J. Catal. 157 (1995) 626.
[3] P. Mériaudeau, C. Naccache, A. Thangaraj, C.L. Bianchi, R. Carli, S. Narayanan, J. Catal. 152 (1995) 313.
[4] P. Mériaudeau, A. Thangaraj, J.F. Dutel, P. Gelin, C. Naccache, J. Catal. 163 (1996) 338.
[5] E.L. Jablonski, A.A. Castro, O.A. Scelza, S.R. de Miguel, Appl. Catal. A 183 (1999) 189.
[6] T. Romero, B. Arenas, E. Perozo, C. Bolivar, G. Bravo, P. Marcano, C. Scott, M.J. Pérez Zurita, J. Goldwasser, J. Catal. 124 (1990) 281.
[7] F.B. Passos, M. Schmal, M.A. Vannice, J. Catal. 160 (1996) 106.
[8] F.B. Passos, D.A.G. Aranda, M. Schmal, J. Catal. 178 (1998) 478.
[9] J. Llorca, N. Homs, J.L.G. Fierro, J. Sales, P. Ramírez de la Piscina, J. Catal. 166 (1997) 44.
[10] J. Llorca, N. Homs, J. León, J. Sales, J.L.G. Fierro, P. Ramírez de la Piscina, Appl. Catal. A 189 (1999) 77.
[11] J. Llorca, P. Ramírez de la Piscina, J. León, J. Sales, J.L.G. Fierro, N. Homs, Stud. Surf. Sci. Catal. 130 (2000) 2513.
[12] F. Humblot, J.P. Candy, F. le Peltier, B. Didillon, J.M. Basset, J. Catal. 179 (1998) 459.
[13] C.D. Wagner, L.E. Davis, M.V. Zeller, J.A. Taylor, R.H. Raymond, L.H. Gale, Surf. Interface Anal. 3 (1981) 211.
[14] J. Llorca, P. Ramírez de la Piscina, J.L.G. Fierro, J. Sales, N. Homs, J. Mol. Catal. A 118 (1997) 101.
[15] M. Primet, J. Catal. 88 (1984) 273.
[16] J. Llorca, N. Homs, J. Araña, J. Sales, P. Ramírez de la Piscina, Appl. Surf. Sci. 134 (1998) 217.
[17] R.A. Dalla Betta, J. Phys. Chem. 79 (1975) 2519.